Reduction methods for the dynamic analysis of substructure models of lighweight building structures

Flodén, Ola; Persson, Kent; Sandberg, Göran

Published in:
Computers & Structures

DOI:
10.1016/j.compstruc.2014.02.011

2014

Reduction methods for the dynamic analysis of substructure models of lightweight building structures

Ola Flodén, Kent Persson, Göran Sandberg
Lund University, Department of Construction Sciences, P.O. Box 118, SE-22100 Lund, Sweden

Abstract

In the present study, different model order reduction methods were compared in terms of their effects on the dynamic characteristics of individual building components. A wide variety of methods were employed in two numerical examples, both being models of wooden floor structures, in order to draw conclusions regarding their relative efficiency when applied to models of such structures. It was observed that a comparison of the methods requires the reduced models to be exposed to realistic boundary conditions, free-free eigenvalue analyses being insufficient for evaluating the accuracy of the reduced models when employed in an assembly of substructures.

Keywords: Model order reduction; Finite element modeling; Substructure modeling; Vibration analysis; Lightweight building structures

1 Introduction

Lightweight buildings are often constructed using prefabricated planar or volume elements, often with use of low-stiffness panels mounted on high-stiffness beams. Accurately assessing the dynamic behaviour of these elements when rather high vibration frequencies are involved requires use of finite element (FE) models representing the geometry in considerable detail. Assembling the individual elements of multi-storey lightweight buildings within the framework of global FE models of entire buildings results in very large models, the number of degrees of freedom (dofs) of which easily exceeds the limits of computer capacity, at least for computations to be performed within reasonable lengths of time. The question arises then of how such FE models can be reduced in size while at the same time being able to represent the dynamic characteristics of the building or buildings in question with sufficient accuracy. The method of dividing a large model into components and creating a global model through coupling models of reduced size of each component is referred to as substructuring. In the present study,

low-frequency vibrations in multi-storey lightweight buildings are modelled by adopting a sub-structuring approach.

In recent decades, a number of methods for model order reduction of dynamic problems have been developed within the area of structural mechanics, mode-based methods being the methods most frequently used. Fairly recently, methods originating from control theory, designated here as modern reduction methods, have been employed within structural mechanics. In contrast to mode-based methods which have an explicit physical interpretation, the modern reduction methods are developed from a purely mathematical point of view. Some mode-based methods are implemented in commercial FE software which enables them to be applied to large-scale problems directly. In order to apply other methods to models created in commercial FE software, the system matrices involved need to be exported from the software and be reduced in another environment.

A number of comparative studies have been published in which the performance of different reduction methods has been evaluated, in connection with mechanical engineering problems. In [1] and [2], modern reduction methods were compared with mode-based methods. In [1], a rack consisting of steel beams was used as a numerical example, the reduction methods involved being compared by studying the structural response within the time domain and the Frobenius norm of the transfer function matrix for different load cases. It was concluded that the modern reduction methods produce excellent reduction results and are more effective than mode-based methods are. In [2], a crankshaft of a piston served as a numerical example, the Frobenius norm of the transfer function matrix being used to compare the reduction methods in question. It was concluded that substantial benefits can be achieved by use of the modern reduction methods. In [3], a wide range of methods was compared by studying the eigenfrequencies and eigenmodes of an elastic rod. The modern reduction methods were found to perform better for mechanical problems than several of the classic methods. In [4], however, in which a clamped beam structure served as a numerical example, it was concluded that mode-based methods are better suited for the analysis of multibody systems than modern reduction methods are. The eigenfrequencies and eigenmodes were analysed with different boundary conditions applied at the interface of the reduced models. It was concluded that mode-based methods are less dependent than the modern reduction methods are on variations in the boundary conditions, something which would clearly be an important advantage in multibody dynamics.

In the comparative studies just referred to, conclusions were drawn on the basis of numerical examples involving relatively simple structures. Lightweight floor and wall structures, however, generally have a much more complex geometry, making it difficult to extrapolate the conclusions in question. Also, in the comparative studies referred to, different types of analyses were used for evaluating the performance of the reduction methods employed, this providing diverse information that can be evaluated in a variety of ways. By applying analyses of multiple types to a given numerical example it should be possible to obtain a broader understanding of the behaviour of different reduction methods than a single type of analysis would provide. Moreover, analysing the reduced models with realistic boundary conditions is necessary since the boundary conditions employed can have a strong influence on the performance of different reduction methods, as demonstrated in [4].

The objective of the analyses carried out in the present investigation was to evaluate the performance of a rather wide range of model order reduction methods by comparing their accuracy and computational cost when applied to detailed FE models of floor and wall structures.

The conclusions will be of value in the process of constructing efficient substructure models for vibration analysis of multi-storey lightweight buildings. The reduced models employed are in this paper evaluated in terms of eigenfrequencies and eigenmodes in a free-free state, as well as in terms of vibration transmission behaviour when the structures in question are exposed to realistic boundary conditions, obtained by connecting them with other building components. New insight is offered regarding both the efficiency of the reduction methods when employed in the analysis of complex structures and the effect of applying realistic boundary conditions to the reduced models.

Commercial FE software of different kinds represent convenient tools for both pre- and post-processing, such as in the coupling of substructures and in the visualisation of results. Since some reduction methods reported on in the literature are incompatible with such software, methods of this sort are either excluded from the analyses here or are used in a modified fashion. A broad range of model order reduction methods presented in the literature will be discussed and the theories behind them taken up. The performance of the reduction methods, applied to lightweight building structures, was evaluated for frequencies of less than 100 Hz by studying two numerical examples. The first example is a model of moderate size of a wooden floor structure, a model created in the commercial FE software Abaqus, from which the system matrices were exported to Matlab, in which various of the reduction methods described in Section 2 were employed. The second example is a large and detailed model of an experimental wooden floor structure, analysed with use of model order reduction methods implemented in Abaqus as well as by use of an alternative approach employing structural elements. Although the conclusions presented in this paper are based in principle on the results of the two numerical examples, many wooden floor and wall structures have geometries and materials similar to those of the structures studied in the two examples. Accordingly, the main conclusions arrived at would appear to be applicable to a wide variety of wooden floor and wall structures similar in topology to these two floors.

2 Model order reduction

An FE formulation of a structural dynamics problem results in a linear equation of motion of the following form [5]:

$$\mathbf{M}\ddot{\mathbf{u}} + \mathbf{C}\dot{\mathbf{u}} + \mathbf{K}\mathbf{u} = \mathbf{f}, \tag{1}$$

where $\mathbf{M, C, K} \in \mathbb{R}^{n\times n}$ are the mass, damping and stiffness matrices respectively, $\mathbf{f} = \mathbf{f}(t) \in \mathbb{R}^{n\times 1}$ is the load vector and $\mathbf{u} = \mathbf{u}(t) \in \mathbb{R}^{n\times 1}$ is the state vector which is sought. A dot denotes differentiation with respect to time, t. The objective of model reduction here is to find a system of m dofs in which $m << n$, one which preserves the dynamic characteristics of the full model. The general approach is to approximate the state vector by use of the transformation $\mathbf{u} = \mathbf{T}\mathbf{u}_R$, where $\mathbf{T} \in \mathbb{R}^{n\times m}$ is a transformation matrix and $\mathbf{u}_R \in \mathbb{R}^{m\times 1}$ is a reduced state vector. Applying the transformation in question to Eq. (1) results in

$$\mathbf{M}_R\ddot{\mathbf{u}}_R + \mathbf{C}_R\dot{\mathbf{u}}_R + \mathbf{K}_R\mathbf{u}_R = \mathbf{f}_R, \tag{2}$$

$$\mathbf{M}_R = \mathbf{T}^T\mathbf{M}\mathbf{T}, \quad \mathbf{C}_R = \mathbf{T}^T\mathbf{C}\mathbf{T}, \quad \mathbf{K}_R = \mathbf{T}^T\mathbf{K}\mathbf{T}, \quad \mathbf{f}_R = \mathbf{T}^T\mathbf{f}, \tag{3}$$

where $\mathbf{M}_R, \mathbf{K}_R, \mathbf{C}_R \in \mathbb{R}^{m\times m}$ are the reduced mass, damping and stiffness matrices, respectively, and $\mathbf{f}_R \in \mathbb{R}^{m\times 1}$ is the reduced load vector. In recent decades, many different methods for model order reduction, involving procedures of varying types for establishing the transformation matrix and the reduced state vector involved, have been proposed in the literature. The dofs in the reduced state vector can be divided into two categories: physical dofs and generalised coordinates. Physical dofs are the dofs of the full system that are retained in the reduction process, whereas the generalised coordinates represent the amplitudes of various Ritz basis vectors [6] that describe the deflection shapes that are allowed in the reduced system. The reduction methods can be categorised according to the type of dofs generated in the reduction process, where *condensation methods* involve only physical dofs, *generalised coordinate methods* are based solely on generalised coordinates, and *hybrid reduction methods* employ a combination of dofs of both types. A number of important methods within each category are listed below.

- Condensation methods
  - Guyan reduction [7]
  - Dynamic reduction [8]
  - Improved reduction system (IRS) [9, 10]
  - System equivalent expansion reduction process (SEREP) [11]
- Generalised coordinate methods
  - Modal truncation [5, 12]
  - Component mode synthesis by Craig–Chang [12, 13]
  - Krylov subspace methods [14, 15]
  - Balanced truncation [16, 17]
- Hybrid methods
  - Component mode synthesis by Craig–Bampton [12, 18]
  - Component mode synthesis by MacNeal [19]
  - Component mode synthesis by Rubin [20]

The methods just referred to, except for the Krylov subspace methods and balanced truncation, which have their origin in control theory and are considered to be modern reduction methods, were developed specifically for structural mechanics. Modal truncation and component mode synthesis by Craig–Chang, Craig–Bampton, Rubin or MacNeal are all mode-based methods, which means that structural eigenmodes of some sort are employed as Ritz basis vectors. In commercial FE software, generalised coordinates are treated as internal dofs and the coupling of substructures is usually realised at the physical dofs by use of Lagrange multipliers [5]. Consequently, if the global model involved is to be analysed and post-processed in commercial FE software, any methods for model order reduction based solely on generalised coordinates are excluded. However, such methods can be combined with condensation methods to obtain hybrid versions of the methods. Component mode synthesis by Craig-Bampton, for example, is modal truncation combined with Guyan reduction. Moreover, variants of component mode synthesis in which Krylov subspace methods instead of modal truncation are combined with Guyan reduction have been described in [21, 22]. Model order reduction methods that result in

reduced models in which the physical dofs at the interfaces are preserved are often referred to as structure-preserving methods.

In the present study, five of the above-listed reduction methods are investigated: Guyan reduction, dynamic reduction, IRS and component mode synthesis, the latter both in the mode-based Craig–Bampton form and in the Krylov subspace version. Out of the mode-based component mode synthesis methods, the Craig–Bampton version, the most commonly employed method among structural engineers, is selected. The Krylov subspace version is included in the studies to investigate the potential improvement in efficiency offered by the increasingly popular methods from control theory when employed for the type of problems studied here. Moreover, modified versions of the component mode synthesis methods are investigated using IRS instead of Guyan reduction as the condensation method, these being referred to as improved component mode synthesis methods [21]. In addition, a set of alternative methods termed generalised methods [23], obtained by deriving the above mentioned methods in a slightly different manner, are investigated.

In the derivations of the reduction methods presented below, the case considered is an undamped one. Since the damping ratio of the structures analysed in the study is relatively low, it has a negligible effect on the eigenfrequencies and the eigenmodes. Also, the damping matrix employed provides only a rough approximation of all the damping phenomena occurring in the structures as a whole. Accordingly, as an alternative to its being reduced in the same way as the mass and stiffness matrices, the damping matrix can be constructed in the reduced system directly.

2.1 Original methods

As mentioned above, the model order reduction methods can be derived in a slightly different manner than in their original versions, this resulting in methods referred to as generalised methods, as presented in Section 2.2. Below, the original versions of the methods investigated here are presented.

Guyan reduction

In the condensation methods, the dofs are separated into masters (m) and slaves (s), the slave dofs being condensed in the reduction process, resulting in a reduced state vector containing only the master dofs. Partitioning the state vector in terms of the master and slave categories enables the system matrices in Eq. (1) to be partitioned into sub-blocks as follows:

$$\begin{bmatrix} \mathbf{M}_{mm} & \mathbf{M}_{ms} \\ \mathbf{M}_{sm} & \mathbf{M}_{ss} \end{bmatrix} \begin{bmatrix} \ddot{\mathbf{u}}_m \\ \ddot{\mathbf{u}}_s \end{bmatrix} + \begin{bmatrix} \mathbf{K}_{mm} & \mathbf{K}_{ms} \\ \mathbf{K}_{sm} & \mathbf{K}_{ss} \end{bmatrix} \begin{bmatrix} \mathbf{u}_m \\ \mathbf{u}_s \end{bmatrix} = \begin{bmatrix} \mathbf{f}_m \\ \mathbf{f}_s \end{bmatrix}. \tag{4}$$

Solving the equation in the second row in Eq. (4) for $\mathbf{u}_s$ results in

$$\mathbf{u}_s = -\mathbf{K}_{ss}^{-1} \left(\mathbf{M}_{sm} \ddot{\mathbf{u}}_m + \mathbf{M}_{ss} \ddot{\mathbf{u}}_s + \mathbf{K}_{sm} \mathbf{u}_m \right), \tag{5}$$

where it has been assumed that there are no loads acting on the slave dofs, so that $\mathbf{f}_s = \mathbf{0}$. Neglecting the inertia terms in Eq. (5) results in the transformation of the state vector for Guyan reduction

$$\begin{bmatrix} \mathbf{u}_m \\ \mathbf{u}_s \end{bmatrix} = \begin{bmatrix} \mathbf{I} \\ -\mathbf{K}_{ss}^{-1} \mathbf{K}_{sm} \end{bmatrix} \mathbf{u}_m = \mathbf{T}_{\text{Guyan}} \mathbf{u}_m, \tag{6}$$

where the transformation matrix $\mathbf{T}_{\text{Guyan}}$ can be used in Eq. (3) to obtain the reduced system matrices and the reduced load vector. Guyan reduction is often referred to as static condensation, since models reduced with Guyan reduction do not result in any errors in static analysis. Due to its static nature, Guyan reduction can be expected to only produce acceptable results for frequencies close to the lowest eigenfrequencies of the system. At higher frequencies, the neglected inertia terms have a stronger influence, resulting in errors of larger size. The performance of this method is highly dependent upon the approach for selecting master dofs. In the numerical examples studied here, only the dofs needed to connect the substructures to the surroundings serve as masters, although additional dofs can be employed as master dofs as well, various methods for selecting such dofs having been proposed [24, 25].

Dynamic reduction

If a harmonic time-dependent load, $\mathbf{f} = \hat{\mathbf{f}} exp(i\omega t)$, is assumed, this results in a harmonic response, $\mathbf{u} = \hat{\mathbf{u}} exp(i\omega t)$, where $i = \sqrt{-1}$ is the imaginary unit, ω is the angular frequency and $\hat{\mathbf{f}}$ and $\hat{\mathbf{u}}$ are the complex load and displacement amplitudes, respectively. Introducing this assumption into Eq. (4) results in the equation of motion applying to the frequency domain

$$\begin{bmatrix} \mathbf{D}_{mm}(\omega) & \mathbf{D}_{ms}(\omega) \\ \mathbf{D}_{sm}(\omega) & \mathbf{D}_{ss}(\omega) \end{bmatrix} \begin{bmatrix} \hat{\mathbf{u}}_m \\ \hat{\mathbf{u}}_s \end{bmatrix} = \begin{bmatrix} \hat{\mathbf{f}}_m \\ \hat{\mathbf{f}}_s \end{bmatrix}, \tag{7}$$

$$\mathbf{D}(\omega) = -\omega^2 \mathbf{M} + \mathbf{K}. \tag{8}$$

Solving the equation in the lower row in Eq. (7) for $\hat{\mathbf{u}}_s$, assuming $\hat{\mathbf{f}}_s = \mathbf{0}$, results in

$$\hat{\mathbf{u}}_s = -\mathbf{D}_{ss}^{-1}(\omega)\, \mathbf{D}_{sm}(\omega)\, \hat{\mathbf{u}}_m, \tag{9}$$

and, consequently, the transformation of the state vector for dynamic reduction is given by

$$\begin{bmatrix} \hat{\mathbf{u}}_m \\ \hat{\mathbf{u}}_s \end{bmatrix} = \begin{bmatrix} \mathbf{I} \\ -\mathbf{D}_{ss}^{-1}(\omega)\, \mathbf{D}_{sm}(\omega) \end{bmatrix} \hat{\mathbf{u}}_m = \mathbf{T}_{\text{Dynamic}} \hat{\mathbf{u}}_m, \tag{10}$$

where the transformation matrix $\mathbf{T}_{\text{Dynamic}}$ requires a selection of ω in order to be established. The special case of dynamic reduction in which $\omega = 0$ results in the transformation of Guyan reduction shown in Eq (6). For harmonic load cases in which the excitation frequency has the same value as ω, dynamic reduction provides exact results. This suggests dynamic reduction to be an effective scheme for analysing a structure subjected to load cases having narrow frequency content. For steady-state analyses, fully accurate reduced models can be obtained by reducing the system matrices at each discrete frequency, yet this is a costly procedure that requires the availability of large memory resources for storing the resulting matrices.

Improved reduction system (IRS)

The term *improved* in the name improved reduction system refers to a perturbation of the transformation taking place in Guyan reduction, Eq. (6). The previously neglected inertia terms are then included as pseudo-static forces. The occurrence of free undamped vibrations of a system reduced by means of a Guyan reduction results in the following expression for the acceleration of the master dofs:

$$\ddot{\mathbf{u}}_m = -\mathbf{M}_{\text{Guyan}}^{-1} \mathbf{K}_{\text{Guyan}} \mathbf{u}_m, \tag{11}$$

where $\mathbf{M}_{\text{Guyan}}$ and $\mathbf{K}_{\text{Guyan}}$ are the reduced stiffness- and mass matrices obtained by employing Guyan reduction. Differentiating Eq. (6) and making use of the relationship expressed in Eq. (11) results in the following expression for acceleration of the slave dofs:

$$\ddot{\mathbf{u}}_s = -\mathbf{K}_{ss}^{-1}\mathbf{K}_{sm}\ddot{\mathbf{u}}_m = \mathbf{K}_{ss}^{-1}\mathbf{K}_{sm}\mathbf{M}_{\text{Guyan}}^{-1}\mathbf{K}_{\text{Guyan}}\mathbf{u}_m. \tag{12}$$

Inserting Eq. (11) and Eq. (12) into Eq. (5) results in the approximation of the slave dofs

$$\mathbf{u}_s = \mathbf{K}_{ss}^{-1}\left(\mathbf{M}_{sm}\mathbf{M}_{\text{Guyan}}^{-1}\mathbf{K}_{\text{Guyan}} - \mathbf{M}_{ss}\mathbf{K}_{ss}^{-1}\mathbf{K}_{sm}\mathbf{M}_{\text{Guyan}}^{-1}\mathbf{K}_{\text{Guyan}} - \mathbf{K}_{sm}\right)\mathbf{u}_m. \tag{13}$$

This rather complicated expression can be written in more compact form so as to obtain the transformation matrix for IRS

$$\mathbf{T}_{\text{IRS}} = \mathbf{T}_{\text{Guyan}} + \mathbf{S}\mathbf{M}\mathbf{T}_{\text{Guyan}}\mathbf{M}_{\text{Guyan}}^{-1}\mathbf{K}_{\text{Guyan}}, \tag{14}$$

$$\mathbf{S} = \begin{bmatrix} \mathbf{0} & \mathbf{0} \\ \mathbf{0} & \mathbf{K}_{ss}^{-1} \end{bmatrix}. \tag{15}$$

In the IRS transformation, the reduced system matrices that Guyan reduction provides are utilised so as to produce updated reduced matrices. As a further extension of this, the updated matrices can be used to create an iterative scheme where the transformation for the ith iteration is given by

$$\mathbf{T}_{\text{IRS},i} = \mathbf{T}_{\text{Guyan}} + \mathbf{S}\mathbf{M}\mathbf{T}_{\text{IRS},i-1}\mathbf{M}_{\text{IRS},i-1}^{-1}\mathbf{K}_{\text{IRS},i-1}, \tag{16}$$

and the iterations are started by calculating $\mathbf{T}_{\text{IRS},1}$ according to Eq. (14). $\mathbf{K}_{\text{IRS},i-1}$ and $\mathbf{M}_{\text{IRS},i-1}$ are the reduced stiffness- and mass matrices of iteration $i-1$, obtained by using $\mathbf{T}_{\text{IRS},i-1}$ in Eq. (3). The iterative scheme converges to form the transformation matrix of SEREP [11], creating a reduced system that reproduces exactly the lowest eigenfrequencies and eigenmodes of the full system. The rate of convergence depends upon the selection of master dofs. In contrast to Guyan reduction, however, IRS does not reproduce the static behaviour of the full system exactly.

Component mode synthesis by Craig–Bampton (CMS)

Use of component mode synthesis by Craig–Bampton, here denoted CMS, compensates for the neglected inertia terms in Guyan reduction through its including a set of generalised coordinates $\boldsymbol{\xi}$. These generalised coordinates represent the amplitudes of a set of eigenmodes for the slave structure, calculated with the master dofs being fixed. Setting $\mathbf{u}_m = \mathbf{0}$ and $\mathbf{f}_s = \mathbf{0}$ in Eq. (4) and assuming a harmonic solution results in the following eigenvalue problem:

$$\mathbf{K}_{ss}\Phi = \lambda\mathbf{M}_{ss}\Phi, \tag{17}$$

which can be solved for the eigenvalues $\lambda = \omega^2$ and the eigenmodes Φ. A number of eigenmodes obtained from Eq. (17), referred to as retained eigenmodes, are selected as additional basis vectors to the approximation of the slave dofs in Eq. (6), resulting in

$$\mathbf{u}_s = -\mathbf{K}_{ss}^{-1}\mathbf{K}_{sm}\mathbf{u}_m + \sum \Phi_i\xi_i = \boldsymbol{\Psi}\mathbf{u}_m + \boldsymbol{\Phi}\boldsymbol{\xi}. \tag{18}$$

This gives the following transformation of the state vector for CMS:

$$\begin{bmatrix} \mathbf{u}_m \\ \mathbf{u}_s \end{bmatrix} = \begin{bmatrix} \mathbf{I} & \mathbf{0} \\ \mathbf{\Psi} & \mathbf{\Phi} \end{bmatrix} \begin{bmatrix} \mathbf{u}_m \\ \boldsymbol{\xi} \end{bmatrix} = \mathbf{T}_{\text{CMS}} \begin{bmatrix} \mathbf{u}_m \\ \boldsymbol{\xi} \end{bmatrix}, \tag{19}$$

which defines the transformation matrix $\mathbf{T}_{\text{CMS}}$. As for Guyan reduction, the accuracy of CMS depends upon the selection of master dofs, this affecting both the static modes and the eigenmodes of the slave structure. Also, the accuracy depends upon the selection of retained eigenmodes, certain eigenmodes having a larger influence than others on the solution of a specific problem. To obtain a reduced model with as great an accuracy for general load distributions as possible, however, all the eigenmodes up to some given limit that is chosen should be included.

Krylov subspace component mode synthesis (KCMS)

The Krylov subspace is defined as

$$K_q\left(\mathbf{A}, \mathbf{b}\right) = span\left\{\mathbf{b}, \mathbf{A}\mathbf{b}, ..., \mathbf{A}^{q-1}\mathbf{b}\right\}, \tag{20}$$

where $\mathbf{A} \in \mathbb{R}^{n \times n}$, $\mathbf{b} \in \mathbb{R}^{n \times 1}$ is called the starting vector and q is a positive integer. $\mathbf{b}$ can also be a block of vectors, in which case each Krylov projection generates a new block of vectors. Since methods originating from control theory are ones developed for systems of an input-output form, the equation of motion is rewritten here as a system of this sort of the following form:

$$\mathbf{M}\ddot{\mathbf{u}} + \mathbf{K}\mathbf{u} = \mathbf{B}\mathbf{x}, \tag{21}$$

$$\mathbf{y} = \mathbf{N}^T\mathbf{u}, \tag{22}$$

where $\mathbf{x} = \mathbf{x}\left(t\right) \in \mathbb{R}^{x \times 1}$ is the input vector, $\mathbf{y} = \mathbf{y}\left(t\right) \in \mathbb{R}^{y \times 1}$ the output vector, $\mathbf{B} \in \mathbb{R}^{n \times x}$ a matrix describing the spatial load distributions and $\mathbf{N} \in \mathbb{R}^{n \times y}$ a matrix relating the state vector to the output vector. A Laplace transformation of the input-output system yields the transfer function $\mathbf{G}(s)$:

$$\mathbf{G}\left(s\right) = \mathbf{N}^T\left(s^2\mathbf{M} + \mathbf{K}\right)^{-1}\mathbf{B}. \tag{23}$$

Krylov subspace methods, which have their origin in the area of control theory, are based on so-called *moment matching*. The moments involved are defined as the coefficients of a Taylor series expansion of $\mathbf{G}(s)$ around $s = 0$. It can be shown that the first q moments of the full system and of a reduced system match if the reduced basis is selected as the Krylov subspace generated by $\mathbf{A} = \mathbf{K}^{-1}\mathbf{M}$ and $\mathbf{b} = \mathbf{K}^{-1}\mathbf{B}$ [15]. In the present study it is required that the reduction methods employed are structure-preserving, i.e. retains the physical dofs at the interfaces. Accordingly, the approach of using Krylov subspace vectors in a component mode synthesis manner, as described in [21, 22], here denoted KCMS, is adopted. Inserting $\mathbf{u}_m = 0$ and $\mathbf{f}_s = \mathbf{B}_s\mathbf{x}_s$ into Eq. (4) results in the following equation of motion for the slave structure:

$$\mathbf{M}_{ss}\ddot{\mathbf{u}}_s + \mathbf{K}_{ss}\mathbf{u}_s = \mathbf{B}_s\mathbf{x}_s. \tag{24}$$

A Krylov subspace is generated for the slave structure by selecting $\mathbf{A} = \mathbf{K}_{ss}^{-1}\mathbf{M}_{ss}$ and $\mathbf{b} = \mathbf{K}_{ss}^{-1}\mathbf{B}_s$:

$$K_q\left(\mathbf{K}_{ss}^{-1}\mathbf{M}_{ss},\mathbf{K}_{ss}^{-1}\mathbf{B}_s\right)=span\left\{\underbrace{\mathbf{K}_{ss}^{-1}\mathbf{B}_s}_{V_{\mathrm{k}}^1},\underbrace{\left(\mathbf{K}_{ss}^{-1}\mathbf{M}_{ss}\right)\mathbf{K}_{ss}^{-1}\mathbf{B}_s}_{V_{\mathrm{k}}^2},...,\underbrace{\left(\mathbf{K}_{ss}^{-1}\mathbf{M}_{ss}\right)^{q-1}\mathbf{K}_{ss}^{-1}\mathbf{B}_s}_{V_{\mathrm{k}}^q}\right\}, \quad (25)$$

and the approximation of the slave dofs in KCMS is given by

$$\mathbf{u}_s=-\mathbf{K}_{ss}^{-1}\mathbf{K}_{sm}\mathbf{u}_m+\sum V_{\mathrm{k}}^i\xi_i=\mathbf{\Psi}\mathbf{u}_m+\mathbf{V}_{\mathrm{k}}\boldsymbol{\xi}, \quad (26)$$

one which is similar to that of component mode synthesis by Craig–Bampton shown in Eq. (18), but with the eigenmodes of the slave structure exchanged for the Krylov subspace vectors as defined in Eq. (25). This results in the transformation of the state vector for KCMS

$$\begin{bmatrix}\mathbf{u}_m\\ \mathbf{u}_s\end{bmatrix}=\begin{bmatrix}\mathbf{I} & \mathbf{0}\\ \mathbf{\Psi} & \mathbf{V}_{\mathrm{k}}\end{bmatrix}\begin{bmatrix}\mathbf{u}_m\\ \boldsymbol{\xi}\end{bmatrix}=\mathbf{T}_{\mathrm{KCMS}}\begin{bmatrix}\mathbf{u}_m\\ \boldsymbol{\xi}\end{bmatrix}, \quad (27)$$

defining the transformation matrix $\mathbf{T}_{\mathrm{KCMS}}$. In order to avoid numerical issues, the Krylov subspace is generated by using the Arnoldi algorithm with modified Gram-Schmidt orthogonalization [14], which creates a set of linearly independent vectors. Calculating the starting vector $\mathbf{b}$ requires that $\mathbf{B}_s$, which describes the spatial load distribution on the slave structure, be selected. In the present study, a substructuring approach for the modelling of multi-storey buildings is adopted. Smaller parts of such buildings are considered as being substructures of these, most of these substructures having no loads that act upon the slave structure. Accordingly, a fictitious load needs to be selected, in the present study a random distribution being used for this.

In contrast to CMS, which includes eigenmodes of the full model as Ritz basis vectors, no eigenvalue extraction is required for creating reduced models by means of the KCMS method. Consequently, it is less costly to create the reduced models employing KCMS and in application where the computation time of this process is of importance, this gives KCMS an advantage over CMS.

Improved component mode synthesis

The two component mode synthesis methods described above are obtained by complementing Guyan reduction by a set of Ritz basis vectors for the slave structure, these being either eigenmodes or Krylov subspace vectors. IRS can be seen as representing an improvement as compared to Guyan reduction, an improvement that can also be applied to the component mode synthesis methods employed here. The transformation matrices of the improved component mode synthesis methods, improved CMS and improved KCMS (ICMS and IKCMS, respectively), can be obtained by simply replacing the basis vectors of Guyan reduction by the basis vectors of IRS:

$$\mathbf{T}_{\mathrm{ICMS}}=\begin{bmatrix}\mathbf{T}_{\mathrm{IRS}} & \hat{\mathbf{\Phi}}\end{bmatrix};\quad \hat{\mathbf{\Phi}}=\begin{bmatrix}\mathbf{0}\\ \mathbf{\Phi}\end{bmatrix}, \quad (28)$$

$$\mathbf{T}_{\mathrm{IKCMS}}=\begin{bmatrix}\mathbf{T}_{\mathrm{IRS}} & \hat{\mathbf{V}}_{\mathrm{k}}\end{bmatrix};\quad \hat{\mathbf{V}}_{\mathrm{k}}=\begin{bmatrix}\mathbf{0}\\ \mathbf{V}_{\mathrm{k}}\end{bmatrix}, \quad (29)$$

where $\mathbf{T}_{\text{IRS}}$ can be given either by the original form of IRS, Eq. (14), or its iterated version, Eq. (16). The use of IRS instead of Guyan reduction can be expected to improve the dynamic behaviour of the reduced models, at the expense of introducing errors in static analyses.

2.2 Generalised methods

The generalised versions of the reduction methods (denoted here by a "g-" in the method names) are obtained by re-formulating the equation of motion. Instead of using the block-partitioning of the system matrices in Eq. (4), the following partitioning is employed:

$$\begin{bmatrix}\mathbf{M}_m & \mathbf{M}_s\end{bmatrix}\begin{bmatrix}\ddot{\mathbf{u}}_m \\ \ddot{\mathbf{u}}_s\end{bmatrix} + \begin{bmatrix}\mathbf{K}_m & \mathbf{K}_s\end{bmatrix}\begin{bmatrix}\mathbf{u}_m \\ \mathbf{u}_s\end{bmatrix} = \begin{bmatrix}\mathbf{f}_m \\ \mathbf{f}_s\end{bmatrix}, \tag{30}$$

with the non-square submatrices $\mathbf{K}_m, \mathbf{M}_m \in \mathbb{R}^{n\times m}$ and $\mathbf{K}_s, \mathbf{M}_s \in \mathbb{R}^{n\times s}$. A drawback of the generalised versions of the methods, in comparison to the original versions, is the increased computational resources needed to construct the reduced models, since this requires the generalised inverses of matrices that are very large.

Generalised Guyan reduction

In the same manner as in Eq. (5) and Eq. (6), the inertia terms in Eq. (30) are neglected when solving for the slave dofs, resulting in the following transformation of the state vector for generalised Guyan (g-Guyan) reduction:

$$\begin{bmatrix}\mathbf{u}_m \\ \mathbf{u}_s\end{bmatrix} = \begin{bmatrix}\mathbf{I} \\ -\mathbf{K}_s^{+}\mathbf{K}_m\end{bmatrix}\mathbf{u}_m = \mathbf{T}_{\text{g-Guyan}}\mathbf{u}_m, \tag{31}$$

where $\mathbf{K}_s^{+} = \left(\mathbf{K}_s^T\mathbf{K}_s\right)^{-1}\mathbf{K}_s^T$ is the generalised left-inverse of $\mathbf{K}_s$ and $\mathbf{T}_{\text{g-Guyan}}$ is the transformation matrix. Note that in the approximation of the slave dofs it is assumed that there are no loads that act on either the master dofs or the slave dofs, $\mathbf{f}_m = \mathbf{0}$ and $\mathbf{f}_s = \mathbf{0}$, respectively, in contrast to the original Guyan reduction, in which only $\mathbf{f}_s = \mathbf{0}$ needs to be assumed.

Generalised dynamic reduction

Through use of an approach corresponding to the derivation of g-Guyan reduction, the transformation matrix of generalised dynamic (g-dynamic) reduction, $\mathbf{T}_{\text{g-Dynamic}}$, can be defined as

$$\begin{bmatrix}\hat{\mathbf{u}}_m \\ \hat{\mathbf{u}}_s\end{bmatrix} = \begin{bmatrix}\mathbf{I} \\ -\mathbf{D}_s^{+}(\omega)\,\mathbf{D}_m(\omega)\end{bmatrix}\hat{\mathbf{u}}_m = \mathbf{T}_{\text{g-Dynamic}}\hat{\mathbf{u}}_m, \tag{32}$$

where $\mathbf{D}_s(\omega) = -\omega^2\mathbf{M}_s + \mathbf{K}_s$ and $\mathbf{D}_m(\omega) = -\omega^2\mathbf{M}_m + \mathbf{K}_m$.

Generalised improved reduction system (g-IRS)

The transformation matrix of generalised IRS is obtained by including the inertia terms found in Eq. (30) as pseudo-static forces, using approximations corresponding to those employed in Eq. (11) and Eq. (12), resulting in

$$\mathbf{T}_{\text{g-IRS}} = \mathbf{T}_{\text{g-Guyan}} + \hat{\mathbf{S}}\mathbf{M}\mathbf{T}_{\text{g-Guyan}}\mathbf{M}_{\text{g-Guyan}}^{-1}\mathbf{K}_{\text{g-Guyan}}, \tag{33}$$

$$\hat{\mathbf{S}} = \begin{bmatrix}\mathbf{0} \\ \mathbf{K}_s^{+}\end{bmatrix}, \tag{34}$$

where $\mathbf{M}_{\text{Guyan}}$ and $\mathbf{K}_{\text{Guyan}}$ are the reduced stiffness- and mass matrices obtained by employing g-Guyan reduction. g-IRS can also be extended to produce an iterative scheme in the same manner as in the original IRS, where the transformation matrix for the ith iteration is given by

$$\mathbf{T}_{\text{g-IRS},i+1} = \mathbf{T}_{\text{g-Guyan}} + \hat{\mathbf{S}}\mathbf{M}\mathbf{T}_{\text{g-IRS},i}\mathbf{M}_{\text{g-IRS},i}^{-1}\mathbf{K}_{\text{g-IRS},i}, \tag{35}$$

and the iterations are started by calculating $\mathbf{T}_{\text{g-IRS},1}$ according to Eq. (33).

Generalised component mode synthesis

The generalised versions of Guyan reduction and IRS can be used to obtain the transformation matrices for the generalised versions of CMS, KCMS, ICMS and IKCMS (g-CMS, g-KCMS, g-ICMS and g-IKCMS, respectively)

$$\mathbf{T}_{\text{g-CMS}} = \begin{bmatrix} \mathbf{T}_{\text{g-Guyan}} & \hat{\mathbf{\Phi}} \end{bmatrix}, \tag{36}$$

$$\mathbf{T}_{\text{g-KCMS}} = \begin{bmatrix} \mathbf{T}_{\text{g-Guyan}} & \hat{\mathbf{V}}_{\text{k}} \end{bmatrix}, \tag{37}$$

$$\mathbf{T}_{\text{g-ICMS}} = \begin{bmatrix} \mathbf{T}_{\text{g-IRS}} & \hat{\mathbf{\Phi}} \end{bmatrix}, \tag{38}$$

$$\mathbf{T}_{\text{g-IKCMS}} = \begin{bmatrix} \mathbf{T}_{\text{g-IRS}} & \hat{\mathbf{V}}_{\text{k}} \end{bmatrix}, \tag{39}$$

where $\hat{\mathbf{\Phi}}$ and $\hat{\mathbf{V}}_{\text{k}}$ are defined in Eq. (28) and Eq. (29), respectively.

2.3 Summary of methods

Table 1 summarises the methods for model order reduction which are presented above and investigated in the numerical examples.

3 Numerical examples

This section considers two numerical examples in which different model order reduction methods are applied to FE models of wooden floor structures. In the first example, a model of moderate size created in Abaqus is studied. The system matrices were exported to Matlab, where the reduction methods described in Section 2 were employed, the reduced models that resulted being analysed. The second example concerns a large and detailed model that was both created and analysed in Abaqus, using reduction methods implemented in the software together with an alternative approach involving use of structural elements. In both examples, two types of analyses were performed: eigenvalue analysis and steady-state analysis. The eigenvalue analysis was performed in a free-free state, i.e. without any displacements of the physical dofs being prescribed. The rigid body eigenmodes that occur in a free-free state are disregarded in the results that are presented. A steady-state analysis was performed to investigate the vibration transmission found in the reduced floor models when realistic boundary conditions were involved, these being accomplished by connecting the reduced models to the top of a pair of wall panel models. The displacement spectrum for one of the wall panels was analysed when a unit load was applied to the other panel.

Condensation methods	
Method name	**Abbrevation**
Guyan reduction	–
Dynamic reduction	–
Improved reduction system	IRS
Generalised Guyan reduction	g-Guyan reduction
Generalised dynamic reduction	g-dynamic reduction
Generalised IRS	g-IRS
Hybrid methods	
Method name	**Abbrevation**
Component mode synthesis by Craig–Bampton	CMS
Improved CMS	ICMS
Krylov subspace component mode synthesis	KCMS
Improved KCMS	IKCMS
Generalised CMS	g-CMS
Generalised ICMS	g-ICMS
Generalised KCMS	g-KCMS
Generalised IKCMS	g-IKCMS

Table 1: The model order reduction methods presented in Section 2 and investigated in Section 3.

3.1 Error quantities

Both the eigenfrequencies and the eigenmodes of the reduced models were studied in the eigenvalue analysis carried out. The eigenfrequencies were compared with those of the full (non-reduced) model in terms of the normalised relative frequency difference (NRFD) and the eigenmodes with those of the full model in terms of the modal assurance criterion (MAC). To obtain a measure for the displacement spectrum of the whole receiver wall panel in the steady-state analysis, a root mean square (RMS) value for the displacement magnitudes in all the nodes of the panel was calculated for each of the frequency steps.

Normalised relative frequency difference (NRFD)

The NRFD of the ith eigenfrequency is defined as

$$\text{NRFD} = \frac{\left| f_i^{red} - f_i^{full} \right|}{f_i^{full}} \cdot 100, \tag{40}$$

where f_i^{full} is the eigenfrequency of the full model and f_i^{red} is the eigenfrequency of the reduced model. This quotient is multiplied by 100 to obtain the NRFD value as a percentage.

Modal assurance criterion (MAC)

The MAC value for the jth eigenmode of the reduced model, Φ_j^{red}, as compared with the ith eigenmode of the full model, Φ_i^{full}, is defined as

$$\text{MAC} = \frac{\left|(\Phi_j^{red})^T(\Phi_i^{full})\right|^2}{(\Phi_j^{red})^T(\Phi_j^{red})(\Phi_i^{full})^T(\Phi_i^{full})}. \tag{41}$$

The eigenmodes of a reduced model often appear in shifted order as compared with the full model. Accordingly, each of the eigenmodes of a reduced model is compared with each of eigenmodes of the full model, within the frequency range which is specified.

Root mean square (RMS)

For any given excitation frequency f in the steady-state analysis, the RMS value is defined here as

$$U_{RMS}(f) = \sqrt{\frac{1}{n_{dof}} \sum_{i=1}^{n_{dof}} U_i(f)^2}, \tag{42}$$

where $U_i(f)$ is the magnitude of the complex amplitude for the ith displacement dof and n_{dof} is the number of displacement dofs of the receiver wall panel. A normalised error of the RMS value for a reduced model, U_{RMS}^{red}, as compared with the RMS value for the full model, U_{RMS}^{full}, can be calculated as

$$U_{RMS}^{\text{error}}(f) = \frac{\left|U_{RMS}^{red}(f) - U_{RMS}^{full}(f)\right|}{U_{RMS}^{full}(f)} \cdot 100. \tag{43}$$

Calculating the error for each excitation frequency enables an error spectrum to be obtained. Since the error spectra typically fluctuate to a marked degree, the result plots used for comparing the different reduction methods make use of averaged error spectra. The errors are averaged by sweeping a 20 Hz wide window over the frequency range and calculating the mean value of the spectrum inside the window for each frequency. Accordingly, the frequency range of the plots is one of 10-90 Hz.

3.2 Numerical example 1: A moderate-sized floor structure

In the first numerical example, a model of a 2445×4090 mm^2 large floor structure was studied. The structure consisted primarily of five load-bearing wooden beams, using a centre-to-centre distance of the successive beams from one another of 600 mm, supporting a particle board surface. At the two shorter sides of the floor, wooden beams were placed perpendicular to the five beams just referred to, creating a box-like structure. Each of these wood beams had a cross-section of 45×220 mm^2 and was modelled using an orthotropic material model possessing the properties shown in Table 2. The particle board had a thickness of 22 mm and was modelled using an isotropic material model having the properties shown in Table 3. The structure was meshed using 20-node brick elements with quadratic interpolation, resulting in 30,807 dofs.

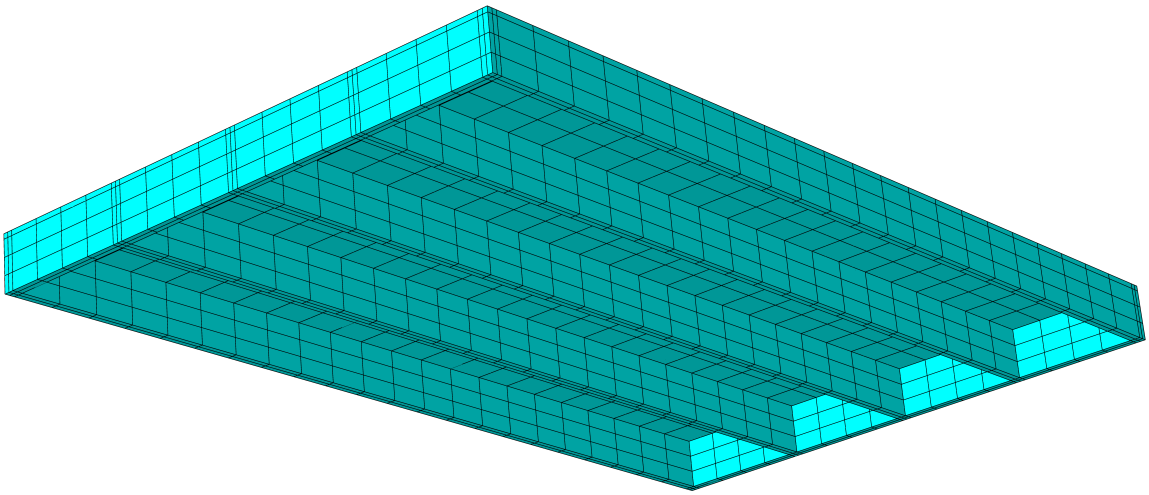

Figure 1: The mesh of the floor structure in numerical example 1.

E_1	E_2	E_3	G_{12}	G_{13}	G_{23}	ν_{12}	ν_{13}	ν_{23}	ρ
8500	350	350	700	700	50	0.2	0.2	0.3	432

Table 2: The material parameters used for the wooden beams [26], the stiffness parameters being given in terms of MPa and the density in kg/m^3.

E	ν	ρ
3000	0.3	767

Table 3: The material parameters used for the particle board [26], the modulus of elasticity being given in terms of MPa and the density in kg/m^3.

The mesh, viewed from below, is shown in Figure 1. The structural components shared mesh nodes at the intersections, the connections thus being modelled as fully interactive.

All the dofs along the centre line on the underside of the outermost beams were selected as master dofs, resulting in there being 576 master dofs altogether, this representing the minimum number of dofs in the reduced models. Reduced models of the full floor-structure model were created by employing the 14 methods for model order reduction listed in Table 1. The dynamic reduction involved a frequency shift of 53.1 Hz, this being the eigenfrequency of the full model closest to 50 Hz, located at the centre of the frequency range. IRS and the improved CMS methods were employed in their iterated versions, using three iterations. A total of 50 generalised coordinates were made use of in the hybrid reduction methods employed. Accordingly, 50 eigenmodes were included in the mode-based methods and 50 Krylov vectors in the Krylov-based methods, resulting in reduced models having 626 dofs.

The reduced models established by employing all of the reduction methods listed in Table 1 resulted in very similar computation times, the condensation methods resulting in marginally shorter times compared to the component mode synthesis methods. The similarity can be explained by the size of the reduced models being similar and the band width of the matrices being very large for all methods. The computation time for the eigenvalue analysis of each of the reduced models was approximately $3\ \%$ of the computation time for the full model.

3.2.1 Eigenvalue analysis

The NRFD values for the original methods are shown in Figure 2, 19 eigenfrequencies being included there, this being the number of eigenfrequencies of less than 100 Hz contained in the full model. The red, yellow and green dashed lines in the figure represent the error levels 10 %, 1 % and 0.1 %, respectively. Guyan reduction provides an acceptable accuracy only for the first eigenfrequency of the full model, whereas dynamic reduction yields high NRFD values for each of the eigenfrequencies. CMS and KCMS provide relatively good and very similar results, the improved variants of both methods increasing the performance appreciably due to the high degree of accuracy of iterated IRS, quite to be expected since the eigenfrequencies iterated IRS provides converge in such a way as to reproduce the eigenfrequencies of the full model exactly.

The NRFD values for the generalised methods are shown in Figure 3. As is evident there, the generalised versions of Guyan reduction and dynamic reduction improve the accuracy as compared with the original versions. The accuracy of IRS decreases for the lower frequencies when its generalised version is employed and, consequently, the accuracy of ICMS and IKCMS decreases as well. The results obtained when employing CMS and KCMS are slightly improved, however, when use is made of the generalised versions of the two.

In Figure 4, the MAC values for the seven original methods and for the generalised versions of Guyan reduction, dynamic reduction, CMS and KCMS are shown. A plot comparing the full model with itself is included in order to demonstrate the orthogonality properties of the eigenmodes. Since the eigenmodes are non-orthogonal in the dot product, the off-diagonal terms are not generally zero in value, although this is the case in the example given here (within the discretization of the MAC plots, the off-diagonal terms being less than 0.1). In agreement with the NRFD results, the MAC values for the original versions of the Guyan reduction and the dynamic reduction correlate poorly with the full model, whereas the generalised versions show a relatively high degree of accuracy. All of the other original reduction methods, except for CMS, show a high degree of correlation with the full model for each of the eigenmodes.

3.2.2 Steady-state analysis

The setup for the steady-state analysis is shown in Figure 5. The floor models were connected to the top of two wall panels, the one a source panel and the other a receiver panel, supporting each end of the load-bearing beams. The wall panels were modelled as shells provided with beam stiffeners at successive spacings from one another of 600 mm each, representing a 2500 mm high wood-framed wall having a plaster board surface. The floor models were tied to the displacement dofs of the wall panels by use of Lagrange multipliers, the bottom edge of the wall panels being fixed. A unit point load in all three directions, shown by the yellow arrows in the figure, was applied to the source panel. The displacements of the receiver wall panel were evaluated in accordance with Eq. (42) for excitation frequencies of up to 100 Hz.

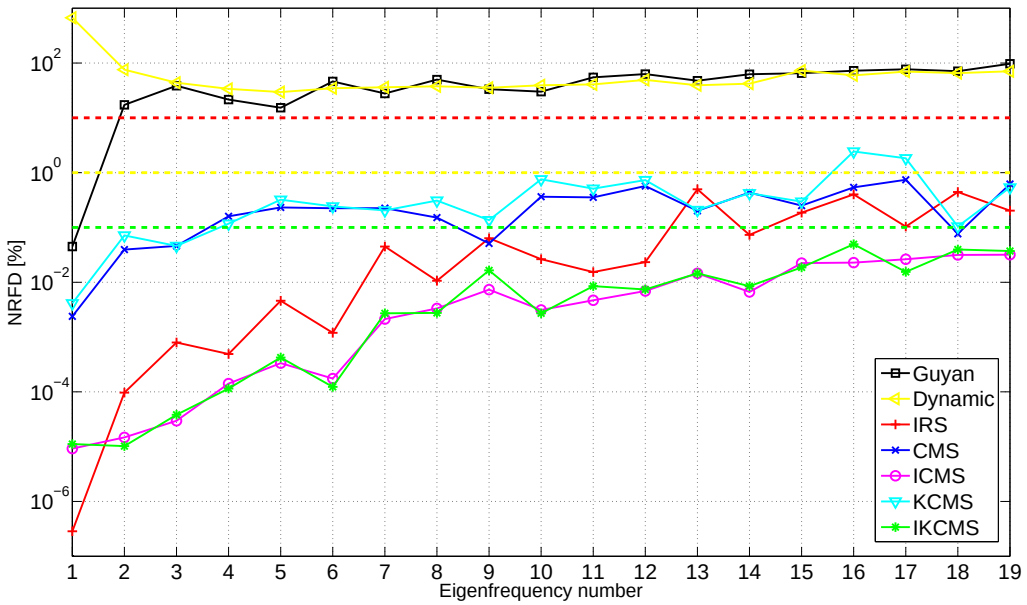

Figure 2: NRFD values for the original model order reduction methods applied to numerical example 1.

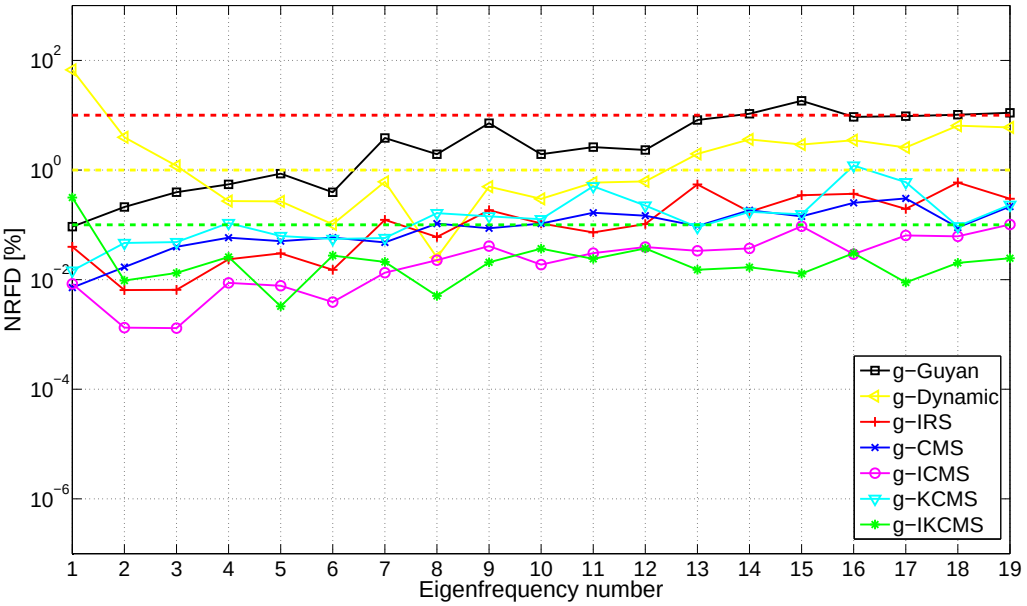

Figure 3: NRFD values for the generalised model order reduction methods applied to numerical example 1.

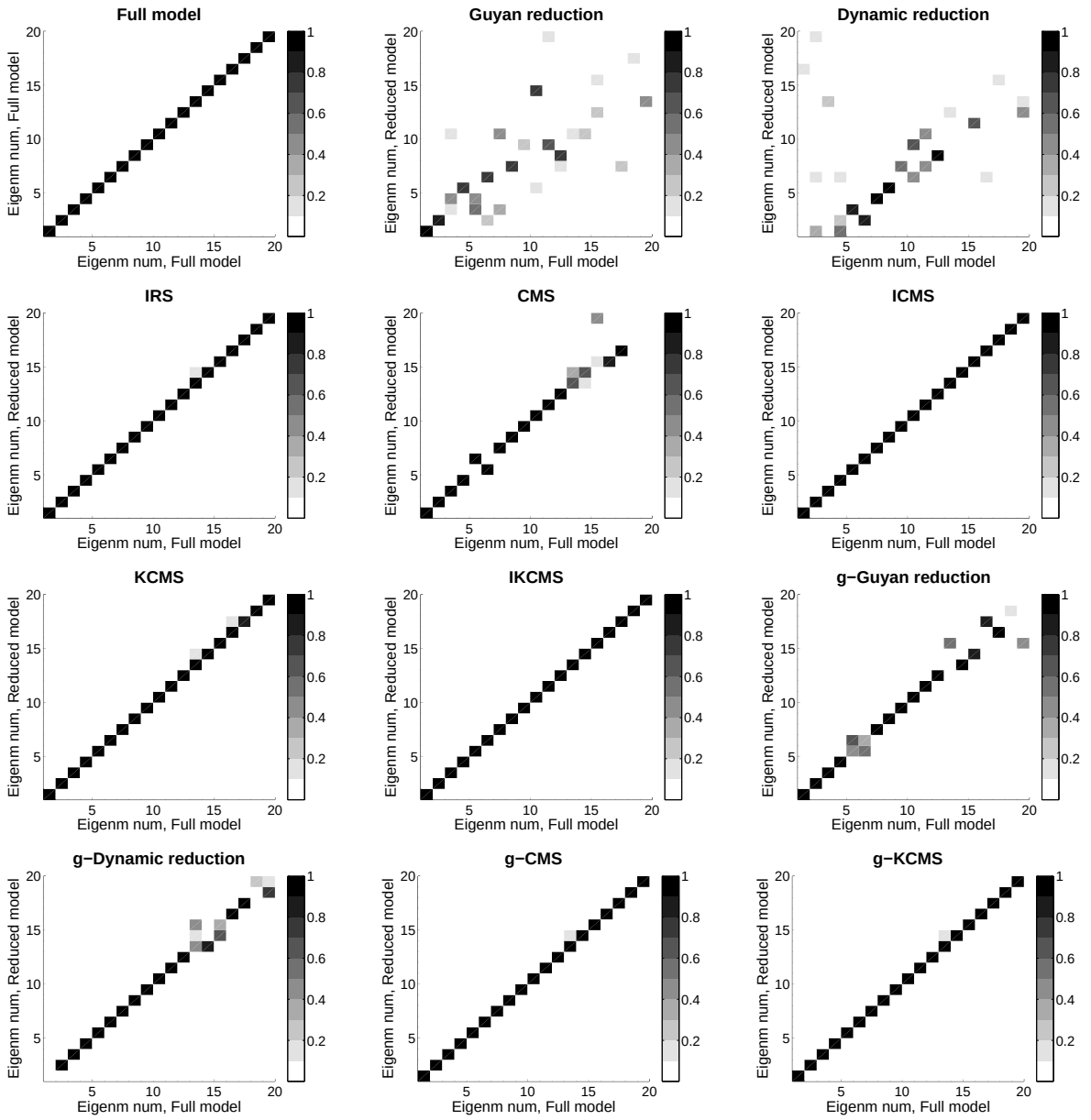

Figure 4: MAC values for the different model order reduction methods applied to numerical example 1.

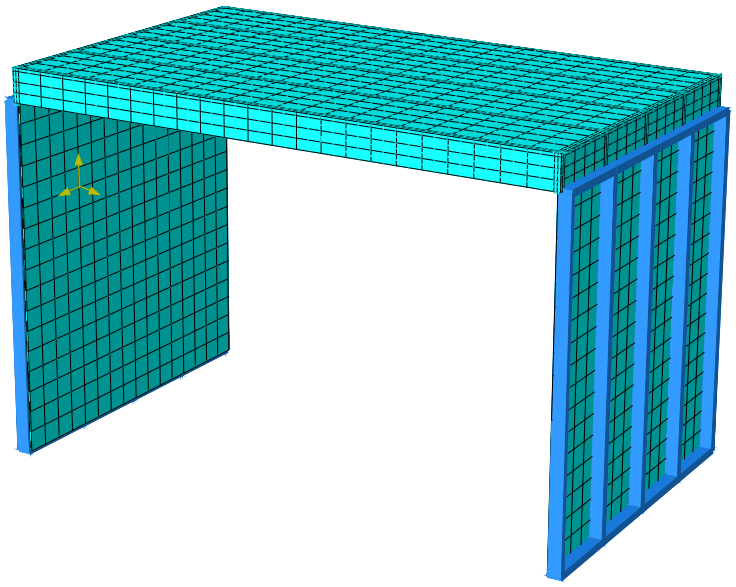

Figure 5: The setup for the steady-state analysis in numerical example 1.

The averaged error of the RMS values obtained using the original methods and the generalised methods is shown in Figure 6 and Figure 7, respectively. The dashed black line in both figures indicates the 10 % error level. In studying Figure 6, one can note that the frequency shift in dynamic reduction strongly affect the performance. Whereas Guyan reduction (corresponding to a 0 Hz shift) generates lower errors when the frequencies involved are lower, dynamic reduction results in the degree of errors being lowest at around 50 Hz, close to the frequency shift selected. CMS and KCMS can be seen to behave very similarly at the higher frequencies, whereas at the lower frequencies the latter is more accurate. In contrast to the results of the eigenvalue analysis, ICMS and IKCMS lower the level of performance for most frequencies as compared with conventional CMS and KCMS. In Figure 7, one can note that the accuracy of Guyan reduction and of dynamic reduction is appreciably greater with use of the generalised versions of these. The accuracy of KCMS decreases markedly at lower frequencies and increases at the higher frequencies when the generalised version of it is employed. As can be seen by comparing the results in Figure 6 and Figure 7, there is, generally speaking, a lesser degree of spread among the results for the different reduction methods when their generalised versions are employed.

In Table 4, the maximum and the mean errors for the frequency range as a whole (without averaging) are shown for both the original and the generalised methods. As is evident, using the generalised versions only has a strong positive effect in the case of Guyan reduction and of dynamic reduction. For most of the hybrid methods, use of the generalised versions leads to a reduction in performance. Of all the reduction methods, it is KCMS that provides the most accurate results in terms both of average and of maximum error levels.

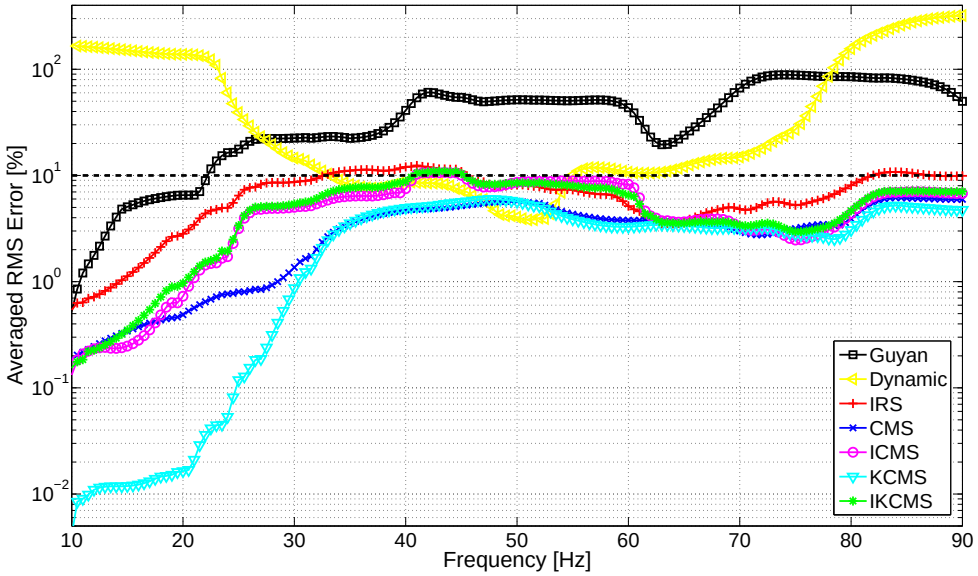

Figure 6: Averaged errors of the RMS values for numerical example 1, as determined with use of the original model order reduction methods.

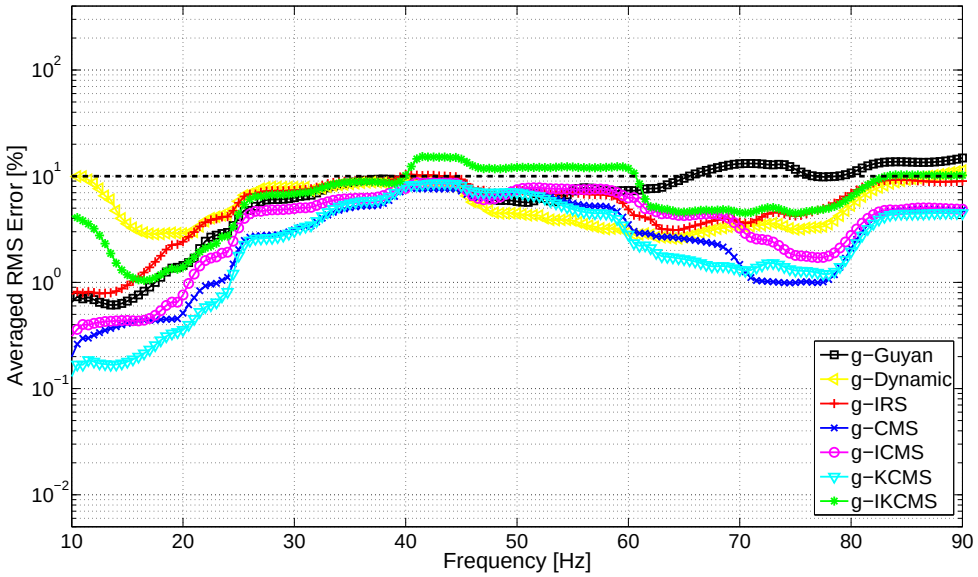

Figure 7: Averaged errors of the RMS values for numerical example 1, as determined with use of the generalised model order reduction methods.

Model	Mean error [%]	Maximum error [%]
Guyan reduction	37.7	276
g-Guyan reduction	8.26	35.0
Dynamic reduction	106	1120
g-dynamic reduction	7.49	54.6
IRS	6.52	39.4
g-IRS	5.70	37.5
CMS	3.26	20.9
g-CMS	3.35	27.0
ICMS	4.81	63.4
g-ICMS	4.18	33.9
KCMS	2.92	20.2
g-KCMS	3.21	27.8
IKCMS	4.96	42.6
g-IKCMS	7.67	98.1

Table 4: Average and maximum error levels of the RMS values obtained for the reduction methods applied to numerical example 1.

3.3 Numerical example 2: A large two-span floor structure

In the second numerical example, a model of an experimental floor structure that was compared with measurements in [26] was studied. The 3645×9045 mm^2 large floor structure consists of seven load-bearing wooden beams, at a centre-to-centre distance of the successive beams from one another of 600 mm, supporting a particle board surface, secondary spaced boarding being attached to the underside of the beams. In the FE model, the wooden beams were placed perpendicular to the load-bearing beams at the two short sides of the floor, creating a box-like structure, in contrast to the experimental structure in which the ends of the beams were free. Each of the wooden beams had a cross-section of 45×220 mm^2 and was modelled using an orthotropic material model having the properties shown in Table 2. The secondary spaced boarding had a cross-section of 28×70 mm^2 and was modelled as having the same material properties as the wooden beams. The particle board had a thickness of 22 mm and was modelled using an isotropic material model possessing the properties shown in Table 3. The structure was meshed using 20-node brick elements with quadratic interpolation, resulting in 632,820 dofs. The mesh, as viewed from below, is shown in Figure 8. The structural components shared mesh nodes at the intersections, the connections thus being modelled as fully interactive.

For reasons of efficiency, it is desirable to connect the floor structure to other structures at discrete points so as to minimise the number of physical dofs retained in the reduced models. Discrete point connections require that rotational dofs fulfil conditions of compatibility. To create rotational coupling in the case of the solid elements, 173 additional nodes, indicated by the yellow crosses in Figure 8, having both displacement dofs and rotational dofs, were created.

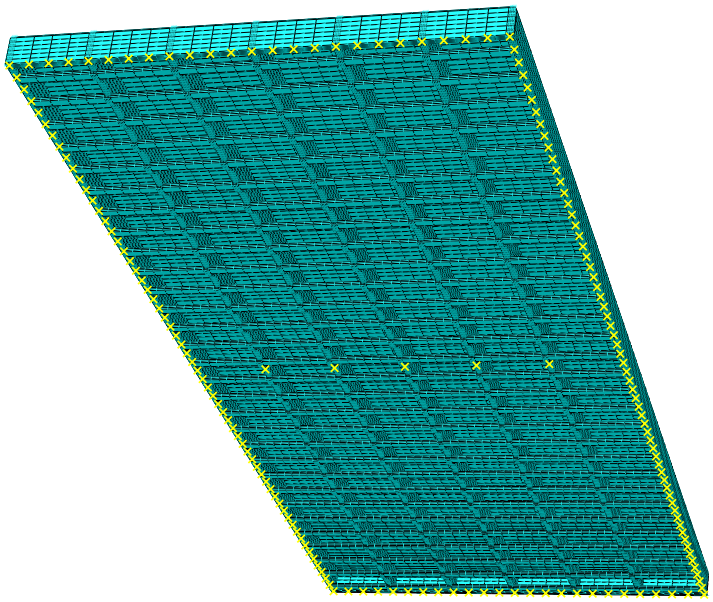

Figure 8: The mesh of the floor structure model in numerical example 2.

These nodes were connected to the neighbouring mesh nodes under conditions of rigid beam constraints, the rotational dofs thus being connected to the rotations of the structure as a whole. The experimental structure has both a mid-span support and end supports. To provide for a modelling of all of the supports, the model has additional nodes possessing rotational dofs both along the underside of the outermost beams and at the middle of the load-bearing beams. The dofs at the 173 additional nodes served as master dofs in the model order reduction, resulting in 1038 master dofs. The model was reduced by use of the two model order reduction methods implemented in Abaqus: Guyan reduction and CMS. The number of eigenmodes retained in the CMS reduction was varied so as to study the convergence of errors.

When employing the model order reduction methods, computationally effective models are obtained by reducing the size of the large system matrices obtained by use of detailed FE models. As an alternative, smaller systems can be constructed directly by use of structural finite elements, beam or shell elements, for example, assumptions being made regarding the kinematic relations and the equilibrium equations involved. These assumptions can turn out to have no more than a negligible effect in static analysis if one or two dimensions of the structure are significantly smaller than the other or others. In dynamic analysis, however, the constraints implied by beam and shell theory can have a strong effect on the structural behaviour in the case of higher frequencies. A structural FE model of the floor structure was created by modelling the panels and the wooden beams in terms of Reissner-Mindlin shell elements, and the secondary spaced boarding in terms of Timoshenko beam elements. The two theories involved allow for shear deformation of the normal to the shell plane and of the beam axis, respectively. Further discussion of the beam and the shell theory can be found in e.g. [5, 27]. The structural-element model was meshed with 720 beam elements and 3,312 shell elements, resulting in 24,762 dofs.

Table 5 shows the size (number of dofs) of the reduced models as well as the computation times obtained for a Lanczos eigenvalue analysis of the 55 first eigenmodes and a steady-state

Model	**Size** (number of dofs)	**Time [s]** (eigenvalue anal.)	**Time [s]** (steady-state anal.)
Full model	632820	590	220000
Structural elements	24762	7.6	1200
Guyan reduction	1038	3.1	410
CMS, 10 re*	1048	3.2	410
CMS, 20 re*	1058	3.2	410
CMS, 50 re*	1088	3.7	420
CMS, 100 re*	1138	5.5	440
CMS, 200 re*	1238	5.7	480
CMS, 500 re*	1538	8.5	620
CMS, 1000 re*	2038	15	970

Table 5: The size and computation times, both for eigenvalue analyses and steady-state analyses, of the reduced models analysed in connection with numerical example 2, the analyses running on one core of an Intel Xeon W3530 CPU of 2.80 GHz, having 10 GB of RAM memory available. *retained eigenmodes

analysis involving 200 steps. The analyses were carried out employing Abaqus/Standard. It can be observed that the computation times are affected by increasing the number of eigenmodes retained in the CMS reduction, the retaining of 1000 eigenmodes (a duplication of the number of dofs compared to Guyan reduction) resulting in the computation times being increased significantly. The number of eigenmodes retained is, of course, a trade-off between accuracy and computational cost, the gain in accuracy being illustrated in the analysis results presented below. It is, however, not possible to estimate the number of eigenmodes required for obtaining a certain accuracy without analysing the full model. Moreover, it can be observed that the computation times for both types of analyses of the structural elements model is similar to those for a model reduced with CMS where 500-1000 eigenmodes are retained, in spite of the former model being over 10 times larger. This is a consequence of the transformation of the system matrices involved in model order reduction, destroying the narrow bandwidth of matrices constructed with the FE method.

3.3.1 Eigenvalue analysis

Figure 9 shows the NRFD values for the reduced models, including CMS when 10, 100 and 1000 eigenmodes are retained. The red, yellow and green dashed lines in the figure show the error levels of 10 %, 1 % and 0.1 %, respectively. The results included 55 eigenfrequencies, which is the number of eigenfrequencies of the full model up to 100 Hz. Guyan reduction assesses only the lowest eigenfrequencies of the full model with an acceptable level of accuracy. Use of CMS in which 10 eigenmodes are retained improves the accuracy obtained for the first 20 eigenmodes, but is inaccurate for the remaining eigenmodes. When 100 eigenmodes are retained, relatively accurate results can be obtained for all of the eigenfrequencies, the retaining of

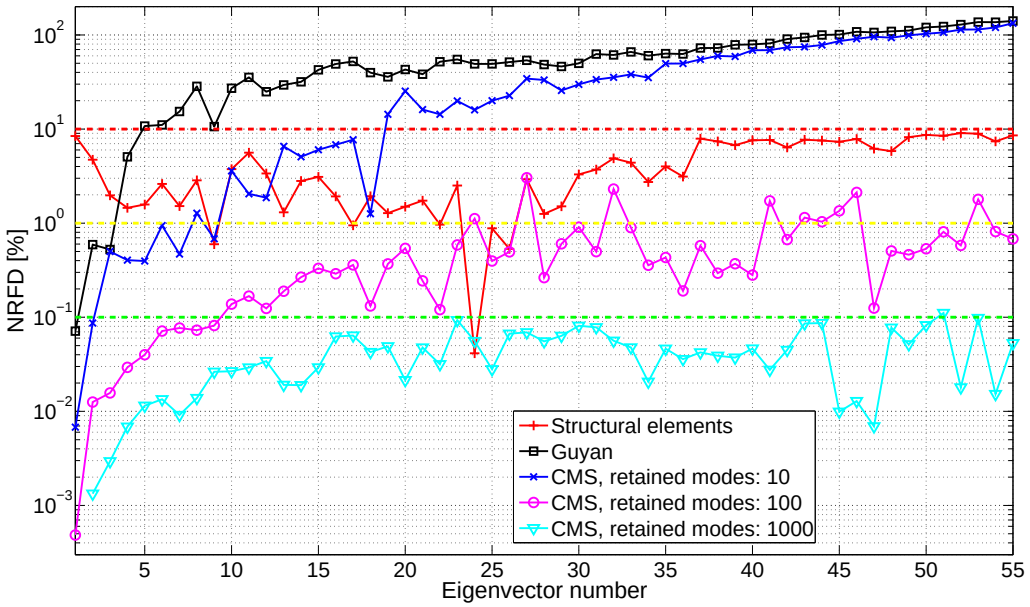

Figure 9: NRFD values for the different reduction methods applied to numerical example 2.

1000 eigenmodes resulting in very small errors. Use of structural elements results in relatively large errors, although the errors are less frequency-dependent than when any of the model order reduction methods are employed.

Figure 4 shows the MAC values obtained with use of the reduced models, including CMS when 10, 50, 100, 500 and 1000 eigenmodes are retained, as well as the full model being compared with itself. For practical reasons, only the master dofs of the reduced models were used for evaluating the eigenmodes. In comparing the plots, it could be noted that the MAC values of the higher eigenmodes were improved with use of CMS when the number of eigenmodes retained was increasing. Whereas Guyan reduction (no eigenmodes retained) only succeeds in modelling a few of the eigenmodes in the full model accurately, the MAC plot for CMS when 1000 eigenmodes are retained is identical to the MAC plot for the full model. The structural element model only models a few of the eigenmodes of the full model with a high degree of accuracy. The correlation there with results of the full model is better for the higher frequencies, however, than is the case of Guyan reduction or CMS when only a few eigenmodes are retained.

3.3.2 Steady-state analysis

The transmission of vibrations was studied using the same approach as in the first numerical example, shown in Figure 5, where the floor models were connected to the top of two wall panels, the one a source panel and the other a receiver panel, supporting each end of the load-bearing beams. The floor models were, in the second numerical example, connected to a third wall panel located at the centre of the floor models through the nodes in the middle of the load-bearing beams. Both the displacement dofs and rotational dofs of the wall panels were linked to the floor models by use of Lagrange multipliers, except in the case of the mid-span wall panel,

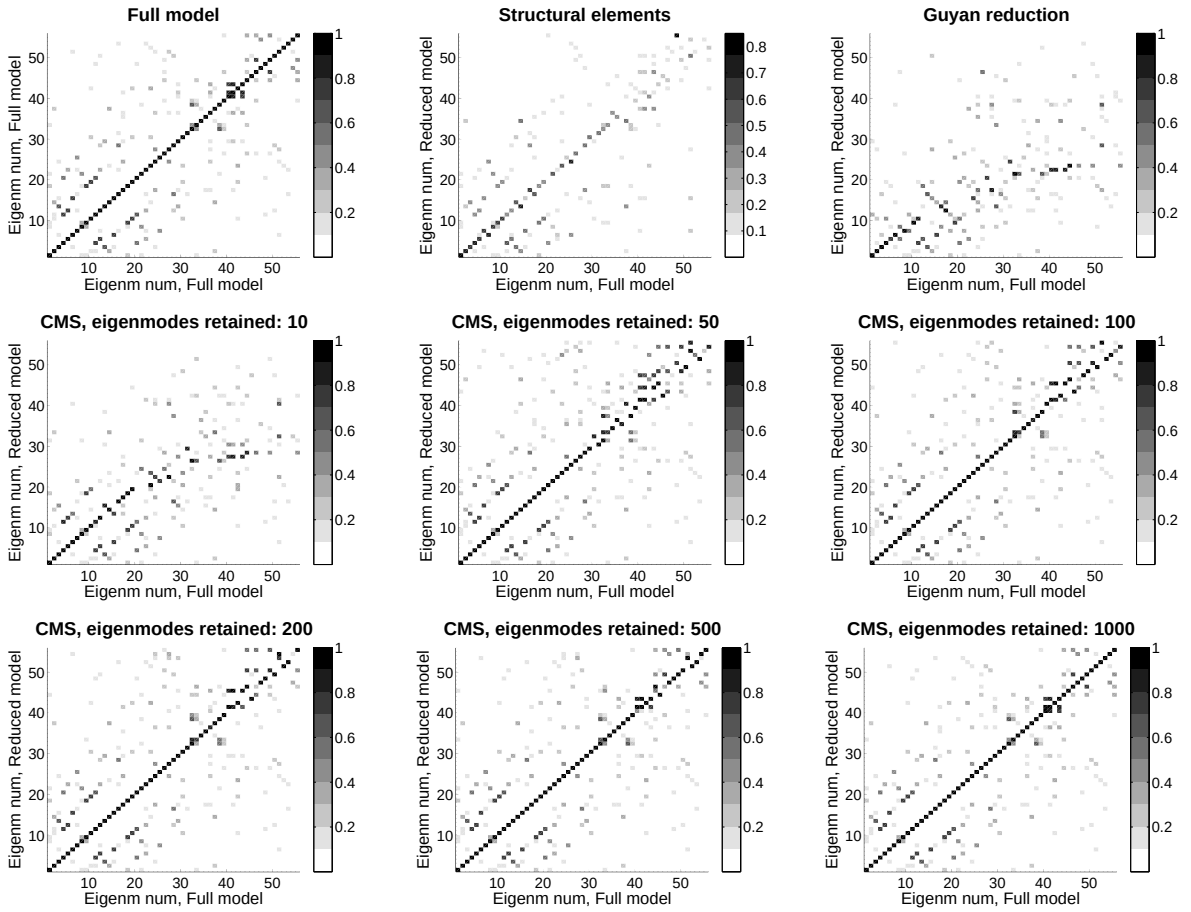

Figure 10: MAC values for the reduction methods employed in connection with numerical example 2.

at which only the displacement dofs were connected. A unit point load in all three directions was applied to the source panel, the displacements at the receiver panel being evaluated for excitation frequencies of up to 100 Hz by use of Eq. (42).

The averaged error of the RMS values for the reduced models, including CMS when 10, 100 and 1000 eigenmodes are retained, is shown in Figure 11. The dashed black line indicates the 10 % error level. Guyan reduction was found to produce large errors for most of the frequencies. Use of CMS in which 10 eigenmodes were retained was found to produce large errors as well, whereas CMS in which 100 eigenmodes were retained was found to be relatively accurate for most of the frequencies. A reduced model in which close to 1000 eigenmodes were retained was needed, however, to obtain satisfactory results for higher frequencies. As in the eigenvalue analysis, the structural element model was found to produce relatively large errors, but with a lesser frequency dependence than for the other methods.

The maximum and the mean error values obtained for the frequency range as a whole (without averaging) are shown in Table 6. As can be seen, the levels of error converge when the number of retained eigenmodes employed in the CMS reduction is increased. When as many as 50 eigenmodes are included, there is a large reduction in the error as compared with Guyan reduction, in spite of the CMS model being only 5 % larger. The convergence is slower when

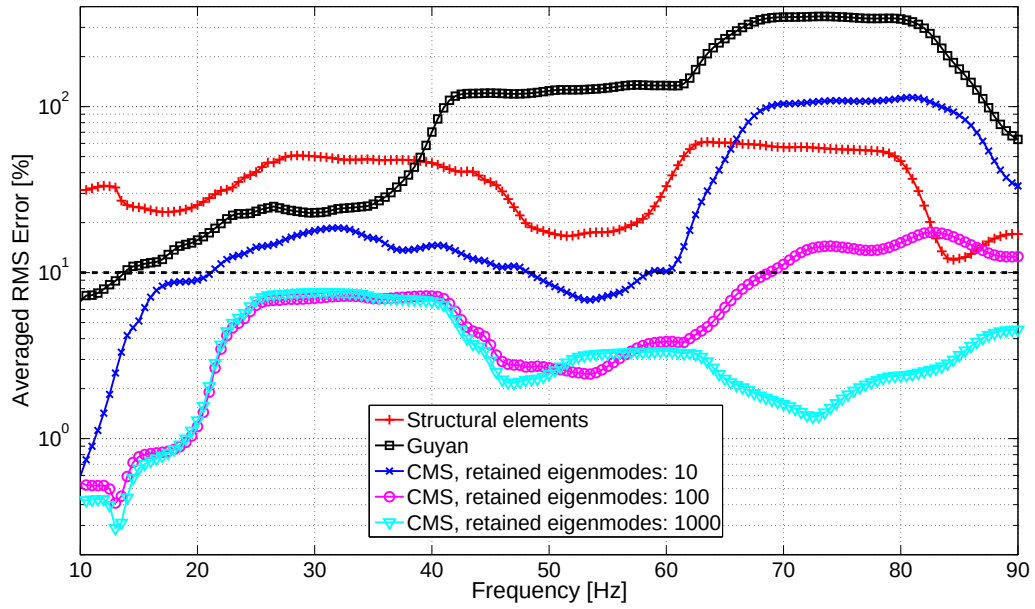

Figure 11: Averaged errors of RMS values obtained for the model order reduction methods used in connection with numerical example 2.

a greater number of eigenmodes are retained, but as shown in Figure 11, at higher frequencies a greater number of eigenmodes are required in order to obtain accurate results. It could also be observed that including a greater number of retained eigenmodes can result in an increase in the maximum error. Consequently, for a given frequency, increasing the number of retained eigenmodes does not necessarily result in a decrease in the level of error involved.

4 Conclusions

The objective of the analyses carried out in the present investigation was to evaluate the performance of a wide range of methods for model order reduction by comparing their accuracy and computational cost when applied to detailed FE models of floor and wall structures. In the first numerical example, it was evident that an eigenvalue analysis of the structure in a free-free state is insufficient for analysing the performance of the different reduction methods. A sensitivity of certain of the reduction methods to boundary conditions was demonstrated, differing observations being made regarding the accuracy of the methods in question in the two analyses: the eigenvalue analysis and the steady-state analysis. This shows the need for the reduced models to be analysed with use of realistic boundary conditions, such as in the case of the steady-state analyses that were considered here.

As was expected, Guyan reduction delivered acceptable results only at frequencies close to the lowest eigenfrequencies of the system, due to the method's static nature. Dynamic reduction was only found to be accurate close to the frequency shift selected and provided inaccurate

Model	Mean error [%]	Maximum error [%]
Structural elements	34.9	61.4
Guyan reduction	113	349
CMS, 10 retained eigenmodes	33.1	114
CMS, 20 retained eigenmodes	11.5	38.4
CMS, 50 retained eigenmodes	7.75	16.3
CMS, 100 retained eigenmodes	6.88	21.4
CMS, 500 retained eigenmodes	3.86	8.92
CMS, 1000 retained eigenmodes	3.38	7.61

Table 6: Average and maximum errors of the RMS values obtained in connection with numerical example 2.

results at frequencies differing to any appreciable extent from this. Iterated improved reduction system (IRS) provided considerably better results than the other condensation methods.

In both numerical examples, component mode synthesis by Craig-Bampton (CMS) proved to be an effective method. The Krylov subspace component mode synthesis (KCMS) method used in the present study was found to be a good alternative as compared with CMS, the two methods offering comparable accuracy. Using IRS to create the improved variants of CMS and KCMS (ICMS and IKCMS, respectively) enabled the accuracy in terms of eigenfrequencies and eigenmodes to be improved appreciably, although at the same time the errors in the steady-state analysis were found to increase, indicating the improved variants to possibly be more sensitive to the boundary conditions introduced in the analysis.

The performance of Guyan reduction and of dynamic reduction was found to clearly be improved by use of the generalised versions of these methods. For the remaining methods, the accuracy was only marginally affected by use of the generalised versions and, for most of the methods, it was decreased at lower frequencies.

The alternative approach of using structural finite elements was found to result in relatively large errors, the computation time, however, being significantly shorter considering the size of the model. The structural element model can, however, be optimised further regarding such matters as the selection of structural element types and the connections involved.

Acknowledgements

The financial support for this work provided by the Silent Spaces project, a part of the EU program Interreg IV A, is gratefully acknowledged.

References

[1] Fehr J., Eberhard P. Simulation process of flexible multibody systems with non-modal model order reduction techniques. Multibody Syst Dyn, 2011;25(3):313-334.

[2] Nowakowski C., Kürschner P., Eberhard P., Benner P. Model reduction of an elastic crankshaft for elastic multibody simulations. J Appl Math and Mech, 2013;93(4):198-216.

[3] Koutsovasilis P., Beitelschmidt M. Comparison of model reduction techniques for large mechanical systems. Multibody Syst Dyn, 2008;20(2):111-128.

[4] Witteveen W. On the modal and non-modal model reduction of metallic structures with variable boundary conditions. World J Mech, 2012;2(6):311-324.

[5] Bathe K.J. Finite element procedures. Prentice Hall, New York, 1996.

[6] Arnold R.R., Citerley R.L. Application of Ritz vectors for dynamic analysis of large structures. Comput Struct, 1985;21(5):901-907.

[7] Guyan R.J. Reduction of stiffness and mass matrices. AIAA J, 1965;3:380.

[8] Leung A.Y.T. An accurate method of dynamic condensation in structural analysis, Int J Numer Methods Eng, 1978;12:1705–1715.

[9] O'Callahan J. A procedure for an improved reduced system (IRS) model. Proc 7th Int Modal Anal Conf, 1989;17–21.

[10] Friswell M.I., Garvey S.D., Penny J.E.T. Model reduction using dynamic and iterated IRS techniques. J Sound Vib, 1995;186:311–323.

[11] O'Callahan J., Avitabile P., Riemer R. System equivalent reduction expansion process (SEREP). Proc 7th Int Modal Anal Conf, 1989;29–37.

[12] Craig R.R. Structural dynamics – An introduction to computer methods. John Wiley & sons Inc., New York, 1981.

[13] Craig R.R., Chang C.J. A review of substructure coupling methods for dynamic analysis. Adv Eng Sci, 1976;2:393-408.

[14] Lohmann B., Salimbahrami B. Introduction to Krylov subspace methods in model order reduction. Methods Appl Autom, 2003;1-13.

[15] Salimbahrami B., Lohmann B. Order reduction of large scale second-order systems using Krylov subspace methods. Linear Algebra Appl, 2006;415(2):385-405.

[16] Benner P. Numerical linear algebra for model reduction in control and simulation. GAMM Mitt, 2006;29(2):275-296.

[17] Reis T., Stykel T. Balanced truncation model reduction of second-order systems. Math Comput Model Dyn Syst, 2008;14(5):391-406.

[18] Craig R.R., Bampton M. Coupling of substructures in dynamic analysis. AIAA J, 1968;6:1313–1319.

[19] MacNeal R.H. A hybrid method of component mode synthesis. Comput Struct, 1971;1(4):581-601.

[20] Rubin S. Improved component-mode representation for structural dynamic analysis. AIAA J, 1975;13:995-1006.

[21] Koutsovasilis P., Beitelschmidt M. Model order reduction of finite element models: improved component mode synthesis. Math Comput Model Dyn Syst, 2010;16(1):57–73.

[22] Häggblad B., Eriksson L. Model reduction methods for dynamic analyses of large structures. Comput Struct, 1993;47(4):735–749.

[23] Koutsovasilis P. Improved component mode synthesis and variants. Multibody Syst Dyn, 2013;29(4):343–359.

[24] Bouhaddi N., Fillod R. A method for selecting master dof in dynamic substructuring using the Guyan condensation method. Comput Struct, 1992;45(5):941-946.

[25] Shah V., Raymund M. Analytical selection of masters for the reduced eigenvalue problem. Int J Numer Methods Eng, 1982;18(1):89–98.

[26] Flodén O., Ejenstam J., Vibration analyses of a wooden floor-wall structure – Experimental and finite element studies. Masters dissertation, Division of Structural Mechanics, Lund University, Sweden, 2011.

[27] Zienkiewicz O.C., Taylor R.L. The finite element method – Fifth edition, Volume 2. MacGraw-Hill, London, 1994.